Published in final edited form as:
Biochemistry. 2011 February 8; 50(5): 820–827. doi:10.1021/bi101483r.

Crosslinking Evidence for Motional Constraints within Chemoreceptor Trimers of Dimers

Diego A. Massazza[1], **John S. Parkinson**[2], and **Claudia A. Studdert**[1,*]

[1]Instituto de Investigaciones Biológicas, Universidad Nacional de Mar del Plata, Mar del Plata, Buenos Aires, Argentina

[2]Biology Department, University of Utah, Salt Lake City, Utah 84112, USA

Abstract

Chemotactic behavior in bacteria relies on the sensing ability of large chemoreceptor clusters that are usually located at the cell pole. In *E. coli*, chemoreceptors show higher order interactions within those clusters based on a trimer-of-dimers organization. This architecture is conserved in a variety of other bacteria and archaea, implying that receptors in many microorganisms form trimer of dimer signaling teams. To gain further insight into the assembly and dynamic behavior of receptor trimers of dimers, we used *in vivo* crosslinking targeted to cysteine residues at various positions that define six different levels along the cytoplasmic signaling domains of the aspartate and serine chemoreceptors, Tar and Tsr. We found that the cytoplasmic domains of these receptors are close to each other near the trimer contact region at the cytoplasmic tip and lie farther apart as the receptor dimers approach the cytoplasmic membrane. Tar and Tsr reporter sites within the same or closely adjacent levels readily formed mixed crosslinks, whereas reporters lying at different distances from the tip did not. These findings indicate that there are no significant vertical displacements of one dimer with respect to the others within the trimer unit. Attractant stimuli had no discernable effect on the crosslinking efficiency of any of the reporters tested, but a strong osmotic stimulus reproducibly enhanced crosslinking at most of the reporter sites, indicating that individual dimers may move closer together under this condition.

Motile bacteria possess sensory systems that enable them to monitor and track chemical gradients in their environment, a behavior known as chemotaxis. The chemotaxis signal transduction pathway has been very well characterized in *E. coli*. See references 1,2 for recent reviews. A multi-protein complex localized at the cell pole monitors attractant and repellent concentrations and transmits signals to the flagellar motors whenever chemoeffector levels change. Attractant increases, for example, trigger signals that promote forward swimming, corresponding to counter-clockwise (CCW) rotation of the flagellar motors. Conversely, repellent increases promote clockwise (CW) motor rotation, which causes the cell to execute random directional changes, or tumbles.

E. coli contains five homodimeric sensory receptors of different detection specificities that are anchored in the cytoplasmic membrane. Four of the receptor types (Tar: aspartate and maltose; Tsr: serine; Tap: dipeptides and pyrimidines; and Trg: ribose and galactose) contain a periplasmic ligand-binding domain delimited, in each subunit, by a pair of transmembrane segments. The fifth receptor, Aer, lacks a periplasmic domain and has instead a cytoplasmic N-terminal FAD-containing PAS domain that receives redox signals from the electron transport chain. The four canonical receptors, collectively known as methyl accepting chemotaxis proteins (MCPs), contain a highly conserved cytoplasmic domain that forms a

*For correspondence: studdert@mdp.edu.ar, Tel. 54 223 4753030 int.12, Fax: 54 223 4753150.

long, four-helix bundle, with membrane-distal hairpin turns in each subunit. Aer, although it is not methylated, shares this feature. The cytoplasmic tips of the receptors bind the histidine kinase CheA and the coupling protein CheW to form ternary signaling complexes whose phosphorylation activity responds to chemoreceptor control. Chemical stimuli elicit rapid changes in CheA activity to trigger locomotor responses, followed by a return of kinase activity to pre-stimulus levels. The sensory adaptation process depends on methylation and demethylation of the receptor signaling domains by an MCP-specific methyltransferase (CheR) and methylesterase (CheB).

The transmission of conformational changes between the sensing and signaling domains of chemoreceptor molecules, as well as the mechanisms of kinase control are still poorly understood. A detailed understanding of the architecture of the ternary signaling complex is necessary to explain the extraordinary sensitivity, high gain, integration of signals and robust adaptation mediated by these relatively simple, yet remarkably efficient, chemoreceptors.

An important clue to the higher-order structure of receptor complexes was provided by a crystal structure of the cytoplasmic domain of *E. coli* Tsr (3). In that structure, three dimeric Tsr fragments were arranged in a trimer-of-dimers organization, with contacts between dimers near the hairpin tip, the region that binds CheW and CheA (4–6). Remarkably, the eleven residues promoting inter-dimer contacts in the trimers are highly conserved in all MCPs and identical in the five *E. coli* chemoreceptors, suggesting that receptors of different types might form mixed trimers of dimers in many prokaryotic chemotaxis systems. *In vivo* crosslinking studies subsequently provided several lines of evidence showing that *E. coli* receptors are indeed organized in trimers of dimers, whose composition depends on the relative abundance of different receptor types in the cell (7,8). Conformational suppression between receptor molecules with amino acid changes in the trimer contact region also showed that trimer formation and dynamics are important factors for proper *in vivo* signaling behavior of receptor arrays (9). Finally, recent electron cryotomography images of receptor clusters in a variety of bacteria and archaea have revealed hexagonal arrays in which the volume and spacing of vertices are consistent with trimers of dimers (10–12).

Thus, multiple lines of evidence support the physiological importance of trimers in receptor signaling. However, alternative receptor-receptor geometries have been proposed, albeit for receptors and signaling complexes under non-native *in vitro* conditions. A cytoplasmic fragment of a *T. maritima* receptor crystallized in a hedgerow arrangement (13). Electron microscopy of a signaling complex assembled with soluble fragments of *E. coli* Tar revealed flattened trimers in a tip-to-tip arrangement (14,15). Solid state NMR studies of receptor-receptor distances in a similar Tar signaling complex suggested that the receptor dimers might be arranged in a parallel fashion inconsistent with a trimer of dimers (16).

In the present study we used a trifunctional thiol crosslinking reagent (TMEA) to test *in vivo* predictions of the trimer of dimers model. In previous work, we employed a cysteine reporter (Tsr-S366C, Tar-S364C) near the receptor's cytoplasmic tip, immediately above the trimer interface region, and found that TMEA trapped about 50% of the receptor subunits in two- and three-subunit crosslinking products, suggesting that TMEA reacts with the axial subunits of receptor dimers organized as trimers (8). Here, we examined TMEA crosslinking of cysteine reporters at different positions along the cytoplasmic domain of Tsr and Tar molecules. We also assessed the possibility of movements of individual dimers within the trimer along its central axis by asking whether different reporters, located at different distances from the tip, can mediate inter-receptor crosslinking. Finally, we tested whether the efficiency of crosslinking depends on the signaling state of receptors. Our results are fully consistent with an *in vivo* trimer of dimers organization for *E. coli* chemoreceptors.

The trimers have tight contacts at their tips that preclude significant movements between receptor dimers along the central axis of the trimer. The decreased efficiency of crosslinking between receptor reporter sites that are farther from the tip indicates that the separation between dimers increases with distance.

Experimental procedures

Bacterial strains

Strains were derivatives of *E. coli* K12 strain RP437 (17) and carried the following genetic markers relevant to the current study: UU1581 [*(flhD-flhB)4 Δ(tsr)-7028 Δ(trg)-100*] and *UU1613 [tar-S364C Δ(tsr)7028 Δ(trg)100 Δ(tap-cheB)2234 Δ(cheA-cheW)2167 zec::Tn10-980*] (18).

Plasmids

Plasmids derived from pACYC184 (19), which confers chloramphenicol resistance, were: pRR31 [salicylate-inducible expression vector] (18), pCS12 [salicylate-inducible wild-type *tsr*] (18), and derivatives of pCS12 encoding Tsr molecules with single-cysteine replacements (ref. 18 and this work).

Plasmids derived from pBR322 (20), which confers ampicillin resistance, were: pNP1 [isopropyl β-D-thiogalactopyranoside (IPTG)-inducible expression vector] (21); and pPA818 [IPTG-inducible *tar-6His*] (P. Ames, personal communication), and single-cysteine containing derivatives (this work). pPA818 encodes a fully functional Tar protein that has a six-histidine tag at its C-terminus.

Site-directed mutagenesis

Mutations in *tsr* or *tar-6His* were introduced with the QuikChange Site-Directed Mutagenesis Kit (Stratagene), using pCS12 or pPA818, respectively, as the template plasmid. Candidate mutants were verified by sequencing the entire chemoreceptor coding region.

TMEA crosslinking assay

Cells were grown at 30°C to mid-log phase in tryptone broth (1% tryptone, 0.5% NaCl), harvested by centrifugation, and resuspended at OD600 = 2 in 10 mM potassium phosphate (pH 7.0), 0.1 mM EDTA. Cell suspensions (0.5 ml) were incubated for 5 min at 30°C and then treated with 50 μM Tris-(2-maleimidoethyl)amine (TMEA, Pierce) for 20 sec at 30°C. Reactions were quenched by the addition of 10 mM *N*-ethylmaleimide. Cells were pelleted and then lysed by boiling in 50 μl of sample buffer (22). Lysate proteins were analyzed by electrophoresis in sodium dodecyl sulfate-containing polyacrylamide gels (SDS-PAGE) as described (8) and visualized by immunoblotting with an antiserum directed against the highly conserved portion of the Tsr signaling domain (4). In some cases, longer gels and with a lower percentage of acrylamide (9%) were used to increase the resolution of mixed crosslinking bands. As secondary antibodies, we used either Cy5-labelled (Amersham) or alkaline phosphatase-conjugated (Sigma) goat anti-rabbit immunoglobulin. Cy5-labelled antibodies were detected with a Storm 840 fluorimager (Amersham); alkaline phosphatase-conjugated antibodies were developed with nitro blue tetrazolium and 5-bromo-4-chloro-3-indolyl phosphate (both from Sigma) and converted to grayscale images with a digital scanner. All gel images were analyzed with ImageQuant software (Amersham).

For analyzing stimulus effects on crosslinking efficiency, cells were washed twice with phosphate buffer before resuspending them at OD600 = 2 in phosphate buffer. Cell suspensions (0.5 ml) were incubated for 5 min at 30°C and then an equal volume of glycerol

(repellent stimulus) was added to bring the final concentration to 1 M immediately before (about ten seconds) the addition of TMEA. For attractant stimulation, 10 mM L-serine or L-aspartate were used. After 20 seconds at 30°C, the reaction was quenched with 10 mM N-ethylmaleimide and samples were processed as described above.

In vivo accessibility of thiol groups

Cells expressing the cysteine-substituted receptors at physiological concentrations were grown to mid-log phase, harvested by centrifugation, and resuspended at OD600 = 2 in 10 mM potassium phosphate (pH 7.0), 0.1 mM EDTA. Cell suspensions (0.5 ml) were treated or not with 5 mM *N*-ethylmaleimide for 15 min at room temperature. Reactions were quenched by the addition of 20 mM dithiotreitol for 15 min at room temperature. Cells were pelleted, washed twice with potassium phosphate buffer to remove excess of dithiotreitol and then lysed by boiling in 50 μl of sample buffer (22). Unblocked thiol groups were then labeled by treatment with 5 mM maleimide-polyethylene glycol (5 kDa) (Boehringer Mannheim) for 15 min at room temperature. Total protein extracts were analyzed by electrophoresis in sodium dodecyl sulfate-containing polyacrylamide gels (SDS-PAGE) as described (8) and visualized by immunoblotting with an antiserum directed against the highly conserved portion of the Tsr signaling domain (4). Gel images were analyzed with ImageQuant software (Amersham), and accessibility of thiol groups was calculated as follows: the percentage of total MCP with shifted mobility in the NEM-treated samples was expressed as a fraction of that percentage in the non-treated cells. This fraction represented the residues that were not accessible for blockage by the NEM treatment. Accessibility could then be expressed as [1 − (fraction of inaccessible residues)]. Accessibility values for residues chosen as controls and calculated from three independent experiments were 0.85 +/− 0.08 (S366C, exposed), and 0.35 +/− 0.17 (T441C, hidden).

Results

TMEA crosslinking sites along the cytoplasmic domains of Tar and Tsr

To assess the native organization of *E. coli* MCP trimers of dimers by cysteine-directed TMEA crosslinking, we constructed single cysteine replacements at various surface residues along the cytoplasmic domain of the Tar and Tsr chemoreceptors. The locations of representative reporter sites are shown in Fig. 1B; the complete list of cysteine replacements is given in Table 1. For simplicity, all residue positions are designated with Tsr numbering (Tar number = [Tsr number −2]), using italic designations for replacements made in Tar.

Near the receptor's cytoplasmic tip one subunit of each dimer, which we designate the axial subunit, resides at the trimer interface; the other, peripheral subunit lies at the outside of the trimer (see cross sections for levels I and II in Fig. 1B). Due to supercoiling of the four-helix cytoplasmic bundle, both axial and peripheral subunits face the trimer axis at longer distances from the tip (see cross sections for levels III to VI in Fig. 1B). We created cysteine replacements at residues that face the central axis of the trimer in the Tsr crystal structure (3), either in the axial or peripheral subunit, depending on their distance from the cytoplasmic tip. We also included one residue, *D345*, whose off-axis location near the trimer interface should preclude efficient crosslinking with its counterparts in the other dimers, unless the reporter sites are able to rotate into more proximal positions within the trimer. Reporter residues were located in both the N-helix, running from the HAMP domain to the tip (residues connected by dark gray lines in Fig. 1B), and in the C-helix, running from the tip to the receptor's C-terminus (residues connected by light gray lines in Fig. 1B). In all, the chosen reporter sites defined six levels, based on cross-section planes through the helix bundle (Fig 1B). Reporters at each level exhibited similar distances from the cytoplasmic

tip, measured from the alpha carbon of the reporter residue to the alpha carbon of residue G390 at the hairpin turn (Table 1).

All cysteine-carrying receptors analyzed in the current study supported full chemotaxis, as assessed in soft agar assays (data not shown). Thus, the overall structure of the marked receptors, including their trimer organization, should closely resemble that of their wild-type counterparts.

TMEA crosslinking efficiency of cysteine reporters from levels I to VI

The TMEA reagent has three thiol-reactive maleimide groups spaced 10.3 Å apart in a trigonal symmetry (see Fig. 2B). TMEA readily permeates into cells and mediates efficient crosslinking of chemoreceptors bearing a cysteine reporter at position 366, generating roughly equal amounts of two- and three-subunit products that together represent about 50% of the receptor subunits (8,18,23). These properties are consistent with the premise that TMEA traps the axial subunits of receptor dimers organized in trimers of dimers.

Based on the Tsr crystal structure, trimers of dimers should pack closely at the receptor tips, but then splay apart as the individual dimers approach the cytoplasmic membrane (see Fig. 1). To test this prediction, we measured TMEA crosslinking efficiencies between cysteine reporters at different distances from the receptor tip. We expressed the marked receptors at physiological levels in cells lacking other receptors and chemotaxis proteins. Previous studies have shown that the CheA and CheW components of ternary signaling complexes have no influence on the pattern or extent of TMEA-mediated receptor crosslinking under these conditions (18). Following TMEA treatment, cells were lysed and whole cell extracts were subjected to gel electrophoresis and immunoblotting using an antibody that recognizes the cytoplasmic domains of Tsr and Tar. To compare the crosslinking efficiencies of different reporter sites, we used receptors with the 366C reporter as internal controls in every experiment. In this way, the amount of three-subunit crosslinking products obtained with any particular reporter could be expressed relative to the level of crosslinking products obtained with the 366C reporter.

To test the possibility that variations in crosslinking efficiencies merely reflect differences in the accessibility of the incorporated thiol groups, we measured the *in vivo* accessibility of every reporter site as described in Methods. Our assay was based on NEM-mediated blockage of thiol groups in intact cells, followed by denaturation and labeling of any unblocked groups by maleimide-polyethylene glycol treatment. All the reporters analyzed in this work showed an accessibility greater than 0.7 in this assay (data not shown). Accordingly, we conclude that differences in crosslinking efficiency mainly reflect differences in reporter site geometry rather than intrinsic reactivity.

We found that the percentage of three-subunit crosslinking products declined with distance of the reporter sites from the cytoplasmic tip (Table 1). Three cysteine residues in level II yielded high levels of three-subunit crosslinking products, about 10–25% of those obtained with the 366C control site in level I. At the opposite extreme, cysteine residues in level VI yielded at most 3% crosslinking products. Cysteine reporters at intermediate levels yielded crosslinking values between those of the level II and level VI reporters. Although the crosslinking behavior of individual reporter sites depends to some extent on their relative orientations, the consistent decline in crosslinking yield with reporter distance from the tip suggests that inter-dimer distances within the trimer increase with distance from the tip. These results indicate that the *in vivo* geometry of receptor trimers is fully consistent with that observed in the crystal structure of the Tsr cytoplasmic domain.

The absence of crosslinking products from the *D345C* reporter (level II, see Table 1) is consistent with the position of this residue in the crystal structure, and suggests that individual dimers may not undergo rotational motions that bring the reporter sites within crosslinking distance. To ask whether attractant stimuli might induce such rotation, we co-expressed Tar-*D345C* and Tsr-T433C receptors (both reporters reside at level II) and stimulated the cells with aspartate or serine immediately before TMEA addition. We did not observe three-subunit products containing Tar-*D345C* subunits (data not shown), which indicates that attractant stimulation does not cause significant rotation of dimers within the trimer.

Effect of reporter geometry on three-subunit crosslinking

In a cell containing Tsr and Tar, two general types of trimers can form: pure trimers, composed exclusively of Tar or Tsr dimers, and mixed trimers containing both types of dimers (Fig. 2A). If both receptors carry a cysteine reporter at the same or closely adjacent level, TMEA should generate both pure and mixed two- and three-subunit crosslinking products (8) (Fig. 2A). Mixed crosslinking products can be detected in low bisacrylamide gels, in which Tar and Tsr subunits have different mobilities (see below).

TMEA treatment of cells expressing Tar E436C (level II) and Tsr E440C (level III) generated both 2- and 3-subunit mixed crosslinking products (Fig. 2C, Table 2). This result conforms to the trimer arrangement in the Tsr crystal structure, because both the distances between reporters (Table 2) and their geometry (Fig. 2B, left panel) are consistent with TMEA-mediated crosslinking.

In contrast, TMEA treatment of cells expressing Tar-V430C (level II) and Tsr-E440C (level III) failed to generate mixed 3-subunit crosslinking products (Fig. 2C, Table 2). Again, this result is consistent with the arrangement of reporters predicted by the Tsr crystal structure. In a mixed trimer of dimers, the three reporter sites would not have an equilateral arrangement and should not be trapped by the same TMEA molecule (Fig. 2B, right panel). However, the calculated distances are compatible with the formation of a two-subunit mixed product (Table 2), and this is what we observed (Fig. 2C). This and the previous result with the off-axis *D345C* reporter argue against any substantial rotation of one dimer with respect to the others in the same trimer.

Assessment of motions between dimers through inter-level crosslinking

The availability of cysteine reporters at different distances from the receptor tip enabled us to test for vertical motions between dimers within a trimer. We reasoned that two different reporter sites farther from the receptor tip than the previously characterized 366 position should generate 2- and 3-subunit crosslinking products, provided that both reporters are at the same level. However, reporter sites in different levels, *e.g.*, Tsr molecules with a reporter at level I and Tar molecules with a reporter at level II, should only give rise to mixed 2- or 3-subunit crosslinking products if dimers undergo displacements relative to one another along the central axis of the trimer (Fig. 3A).

Accordingly, we assessed inter-level crosslinking between reporters in levels I and II, whose distances from the tip differ by about 30 Å (Table 1). We expressed Tsr-S366C (level I) or Tsr-T433C (level II) in cells that contained chromosomally-encoded levels of Tar-*S366C*, treated with TMEA, and analyzed the crosslinking products by immunoblotting (Fig. 3B). As expected, mixed crosslinking products were detected when both receptors carried the 366C reporter (Fig. 3B, left). However, no mixed products were seen when the cysteine reporter in Tsr resided at level II (Fig. 3B, right). It is important to note that Tsr-T433C is incorporated into mixed trimers of dimers, as evidenced by the decrease in pure Tar

crosslinking products as Tsr expression increases and by the fact that pure Tsr three-subunit products are only evident at the highest level of Tsr expression. Thus, the absence of mixed crosslinking products indicates that even though the marked receptors can form mixed trimers, TMEA cannot trap receptor subunits that have reporter residues in different levels. We conclude that, within an assembled trimer, there are no movements of dimers relative to one another that are large enough to allow crosslinking across reporter levels.

In a reciprocal experiment, we expressed Tsr-S366C (level I) or Tsr-T433C (level II) in cells expressing Tar-*V430C* (level II) from a compatible plasmid, and analyzed the crosslinking products after TMEA treatment (Fig. 3D). Again, when both receptors bore reporter sites at the same level (in this case, level II), mixed crosslinking products were seen (Fig. 3D, three right panels). In contrast, with reporter sites at different levels, no mixed crosslinking products were evident (Fig. 3D, three left panels). The presence or absence of mixed crosslinking products is most apparent in the 2-subunit region of the gel, because the corresponding pure crosslinking products (Tar-Tar or Tsr-Tsr) have clearly different mobilities, whereas in the 3-subunit region the crosslinking products for the combination Tar-*V430C*/Tsr-S366C migrate close together and are less easily distinguished by their positions. Note that crosslinked samples of each receptor alone were included in adjacent lanes to show the positions of the pure products. Those positions depend greatly on the location of the cysteine residue.

We also assessed inter-level crosslinking between reporters residing in levels II and V, whose distances from the tip differ by 20 Å (Table 1). Again, no mixed 2- or 3-subunit crosslinking products could be detected in cells expressing Tar-*E436C* and Tsr-S447C (Fig. 3B). We conclude from these experiments that the dimers in a trimer do not move far enough relative to each other to crosslink a cysteine residue in level I to one in level II, or a cysteine residue in level II to one in level V. Given the distances between the corresponding alpha-carbons in the Tsr crystal structure (Table 2), the absence of 2-subunit products argues against the occurrence of significant dimer-dimer movements parallel to the trimer axis.

Effect of signaling state on TMEA-crosslinking efficiency in trimers of dimers

In our original characterization of the Tsr-S366C reporter, we observed that its efficiency of TMEA crosslinking was not influenced by the presence of CheA and/or CheW (at physiological levels), by the receptor's methylation state, or by an attractant stimulus (8). These results indicate that the 366 positions in the axial subunits of a trimer, immediately above the trimer contact region, remain essentially stationary over a range of signaling conditions.

To ask whether cysteine reporters farther from the trimer contact region might move closer or farther apart or change their relative orientation in response to an attractant or repellent stimulus, we analyzed the TMEA crosslinking patterns of receptors with reporter sites at various levels. Cells expressing the marked receptors were treated with various stimuli for five seconds just before adding the TMEA reagent. We found that attractant stimuli did not cause an appreciable difference in crosslinking efficiency for any of the reporters (data not shown). However, glycerol (a repellent stimulus) caused a reproducible increase in crosslinking efficiency for reporters located in levels II to VI (Fig. 4). This finding suggests that the dimers within a trimer move closer together in response to an osmotic stimulus, a behavior previously observed in YFP-tagged receptor molecules by Vaknin and Berg (24,25).

To determine whether this apparent compression of the trimer reflected the signaling state of the receptors, we introduced the reporter T433C (level II) into Tsr molecules bearing mutations that mimicked different methylation states (QEQE, QQQQ, EEEE) or that locked

receptor output in the kinase-off (A413V. ref. 4) or kinase-on [L237R (26), M259T, (Zhou et al., in preparation)] signaling state. All mutant receptors exhibited crosslinking efficiency similar to the wild-type receptor (data not shown). All mutant receptors also displayed the glycerol-enhanced crosslinking behavior observed in the wild-type receptor. Thus, it appears that a strong osmotic stimulus compresses trimers of dimers, but mutations that "lock" the receptor in different signaling states cannot block this response. It is unclear, therefore, whether the glycerol effect is related to receptor signaling.

Discussion

Native organization of MCP trimers of dimers

Our *in vivo* crosslinking results are consistent with a native arrangement of receptors in trimers of dimers that are held together at their cytoplasmic tips and splay apart towards the membrane. Our findings do not support proposed alternative arrangements in which the cytoplasmic domains of neighboring receptors are roughly parallel to each other (15,16). This conclusion is based on a systematic decline in three-subunit TMEA crosslinking efficiency with reporter sites situated at increasing distances from the cytoplasmic tip of the receptor molecule.

The presence or absence of CheA and CheW had no effect on crosslinking efficiency for any of the reporter sites used in this study. This observation suggests that crosslinking yield reflects interactions between dimers within a trimer of dimers rather than inter-trimer interactions, because higher-order interactions between receptors would probably be enhanced by the presence of the scaffolding proteins required to form a stable and tight cluster of chemoreceptors (27,28). The clear absence of crosslinking between receptors carrying cysteine residues at different levels indicates that trimer-stabilizing interactions of the receptor tips do not permit large vertical displacements of one receptor dimer relative to another. This lack of large scale movement holds even in the absence of CheA and CheW, a condition in which dimer exchange between trimers is highly dynamic (18).

Effect of stimuli and signaling state on relative distances between receptor dimers

Attractant stimuli had no significant effect on crosslinking efficiency for any reporter site tested. This result argues against significant stimulus-induced rotational movements of dimers within the trimer, which would have been expected to decrease the yield of three-subunit crosslinking products for reporters facing the central trimer axis. In the case of Tar carrying the off-axis reporter *D345C*, we did not observe any three-subunit crosslinking product for Tar alone or in combination with Tsr molecules carrying cysteine substitutions at the same level, either in the absence or presence of an attractant stimulus. This behavior also argues against rotational motions of dimers within a trimer, regardless of signaling state.

Glycerol, a repellent stimulus, caused a moderate but reproducible increase in crosslinking efficiency at most reporter positions (mainly from levels II to VI), indicating that trimers may be compressed during repellent signaling, as previously suggested by the homo-FRET studies of Vaknin and Berg (24,25). However, this glycerol-induced compression of the trimer does not seem to reflect the signaling state of the receptor, because receptors mutationally locked in the kinase-on state or with activating glutamine residues at all four methylation sites did not show increased crosslinking efficiency. Moreover, glycerol stimuli still enhanced the crosslinking efficiencies of mutationally activated receptors, suggesting that the glycerol effect on trimer structure is different from the conformational change associated with kinase activation.

In summary, our *in vivo* receptor crosslinking studies support the trimer of dimers geometry revealed by the crystal structure of the Tsr signaling domain. Further, there appear to be no

large vertical or rotational shifts between the members of a trimer during chemotactic signaling. We conclude that stimulus-induced changes in the conformation or dynamic behavior of trimer-based signaling teams fall below the resolution of *in vivo* crosslinking methods. In contrast, several studies have reported stimulus-dependent crosslinking effects that probably reflect changes in the arrangement or relative orientation of trimers in a receptor signaling cluster (29–31). How relatively small structural changes within trimers lead to seemingly larger changes in the organization of receptor arrays is key to understanding the mechanism of cooperative signal amplification by chemoreceptors, but remains an open question.

Acknowledgments

This work was supported by a National Institutes of Health Fogarty International Research Collaboration Award (TW007216 to J.S.P. and C.A.S.), by research grant GM19559 (to J.S.P.) from the National Institute of General Medical Sciences, and by research grant 31943 (to C.A.S.) from the Agencia Nacional para la Promoción de la Ciencia y la Tecnología, Argentina.

We thank Hai Pham (University of Utah) and Kika Kitanovic (University of Utah) for helpful scientific and editorial comments on the manuscript.

Abbreviations

IPTG	isopropyl β-D-thiogalactopyranoside
MCP	methyl-accepting chemotaxis protein
NMR	nuclear magnetic resonance
SDS-PAGE	sodium dodecyl sulfate-containing polyacrylamide gel electrophoresis
TMEA	Tris-(2-maleimidoethyl)amine

References

1. Hazelbauer GL, Falke JJ, Parkinson JS. Bacterial chemoreceptors: high-performance signaling in networked arrays. Trends Biochem. Sci. 2008; 33:9–19. [PubMed: 18165013]
2. Hazelbauer GL, Lai WC. Bacterial chemoreceptors: providing enhanced features to two-component signaling. Curr. Opin. Microbiol. 2010; 13:124–132. [PubMed: 20122866]
3. Kim KK, Yokota H, Kim SH. Four-helical-bundle structure of the cytoplasmic domain of a serine chemotaxis receptor. Nature. 1999; 400:787–792. [PubMed: 10466731]
4. Ames P, Parkinson JS. Constitutively signaling fragments of Tsr, the *Escherichia coli* serine chemoreceptor. J. Bacteriol. 1994; 176:6340–6348. [PubMed: 7929006]
5. Ames P, Yu YA, Parkinson JS. Methylation segments are not required for chemotactic signalling by cytoplasmic fragments of Tsr, the methyl-accepting serine chemoreceptor of *Escherichia coli*. Mol. Microbiol. 1996; 19:737–746. [PubMed: 8820644]
6. Zhang P, Khursigara CM, Hartnell LM, Subramaniam S. Direct visualization of *Escherichia coli* chemotaxis receptor arrays using cryo-electron microscopy. Proc. Natl. Acad. Sci. U S A. 2007; 104:3777–3781. [PubMed: 17360429]
7. Ames P, Studdert CA, Reiser RH, Parkinson JS. Collaborative signaling by mixed chemoreceptor teams in *Escherichia coli*. Proc. Natl. Acad. Sci. U S A. 2002; 99:7060–7065. [PubMed: 11983857]
8. Studdert CA, Parkinson JS. Crosslinking snapshots of bacterial chemoreceptor squads. Proc. Natl. Acad. Sci. U S A. 2004; 101:2117–2122. [PubMed: 14769919]
9. Ames P, Parkinson JS. Conformational suppression of inter-receptor signaling defects. Proc. Natl. Acad. Sci. U S A. 2006; 103:9292–9297. [PubMed: 16751275]
10. Khursigara CM, Wu X, Subramaniam S. Chemoreceptors in *Caulobacter crescentus*: trimers of receptor dimers in a partially ordered hexagonally packed array. J. Bacteriol. 2008; 190:6805–6810. [PubMed: 18689468]

11. Briegel A, Ding HJ, Li Z, Werner J, Gitai Z, Dias DP, Jensen RB, Jensen G. Location and architecture of the *Caulobacter crescentus* chemoreceptor array. Mol. Microbiol. 2008; 69:30–41. [PubMed: 18363791]
12. Briegel A, Ortega DR, Tocheva EI, Wuichet K, Li Z, Chen S, Muller A, Iancu CV, Murphy GE, Dobro MJ, Zhulin IB, Jensen GJ. Universal architecture of bacterial chemoreceptor arrays. Proc. Natl. Acad. Sci. U S A. 2009; 106:17181–17186. [PubMed: 19805102]
13. Park SY, Borbat PP, Gonzalez-Bonet G, Bhatnagar J, Pollard AM, Freed JH, Bilwes AM, Crane BR. Reconstruction of the chemotaxis receptor-kinase assembly. Nat. Struct. Mol. Biol. 2006; 13:400–407. [PubMed: 16622408]
14. Francis NR, Levit MN, Shaikh TR, Melanson LA, Stock JB, DeRosier DJ. Subunit organization in a soluble complex of Tar, CheW, and CheA by electron microscopy. J. Biol. Chem. 2002; 277:36755–36759. [PubMed: 12119290]
15. Francis NR, Wolanin PM, Stock JB, Derosier DJ, Thomas DR. Three-dimensional structure and organization of a receptor/signaling complex. Proc. Natl. Acad. Sci. U S A. 2004; 101:17480–17485. [PubMed: 15572451]
16. Fowler DJ, Weis RM, Thompson LK. Kinase-active signaling complexes of bacterial chemoreceptors do not contain proposed receptor-receptor contacts observed in crystal structures. Biochemistry. 2010; 49:1425–1434. [PubMed: 20088541]
17. Parkinson JS, Houts SE. Isolation and behavior of *Escherichia coli* deletion mutants lacking chemotaxis functions. J. Bacteriol. 1982; 151:106–113. [PubMed: 7045071]
18. Studdert CA, Parkinson JS. Insights into the organization and dynamics of bacterial chemoreceptor clusters through *in vivo* crosslinking studies. Proc. Natl. Acad. Sci. U S A. 2005; 102:15623–15628. [PubMed: 16230637]
19. Chang AC, Cohen SN. Construction and characterization of amplifiable multicopy DNA cloning vehicles derived from the P15A cryptic miniplasmid. J. Bacteriol. 1978; 134:1141–1156. [PubMed: 149110]
20. Bolivar F, Rodriguez RL, Greene PJ, Betlach MC, Heyneker HL, Boyer HW. Construction and characterization of new cloning vehicles. II. A multipurpose cloning system. Gene. 1977; 2:95–113. [PubMed: 344137]
21. Bibikov SI, Miller AC, Gosink KK, Parkinson JS. Methylation-independent aerotaxis mediated by the *Escherichia coli* Aer protein. J. Bacteriol. 2004; 186:3730–3737. [PubMed: 15175286]
22. Laemmli UK. Cleavage of structural proteins during the assembly of the head of bacteriophage T4. Nature. 1970; 227:680–685. [PubMed: 5432063]
23. Cardozo M, Massazza D, Parkinson J, Studdert C. Disruption of chemoreceptor signaling arrays by high level of CheW, the receptor-kinase coupling protein. Mol. Microbiol. 2010; 75:1171–1181. [PubMed: 20487303]
24. Vaknin A, Berg HC. Osmotic stress mechanically perturbs chemoreceptors in *Escherichia coli*. Proc. Natl. Acad. Sci. U S A. 2006; 103:592–596. [PubMed: 16407109]
25. Vaknin A, Berg HC. Physical responses of bacterial chemoreceptors. J. Mol. Biol. 2007; 366:1416–1423. [PubMed: 17217957]
26. Ames P, Zhou Q, Parkinson JS. Mutational analysis of the connector segment in the HAMP domain of Tsr, the *Escherichia coli* serine chemoreceptor. J. Bacteriol. 2008; 190:6676–6685. [PubMed: 18621896]
27. Maddock JR, Shapiro L. Polar location of the chemoreceptor complex in the *Escherichia coli* cell. Science. 1993; 259:1717–1723. [PubMed: 8456299]
28. Kentner D, Sourjik V. Spatial organization of the bacterial chemotaxis system. Curr. Opin. Microbiol. 2006; 9:619–624. [PubMed: 17064953]
29. Homma M, Shiomi D, Kawagishi I. Attractant binding alters arrangement of chemoreceptor dimers within its cluster at a cell pole. Proc. Natl. Acad. Sci. U S A. 2004; 101:3462–3467. [PubMed: 14993606]
30. Irieda H, Homma M, Kawagishi I. Control of chemotactic signal gain via modulation of a pre-formed receptor array. J. Biol. Chem. 2006; 281:23880–23886. [PubMed: 16679313]

31. Borrok MJ, Kolonko EM, Kiessling LL. Chemical probes of bacterial signal transduction reveal that repellents stabilize and attractants destabilize the chemoreceptor array. ACS Chem. Biol. 2008; 3:101–109. [PubMed: 18278851]

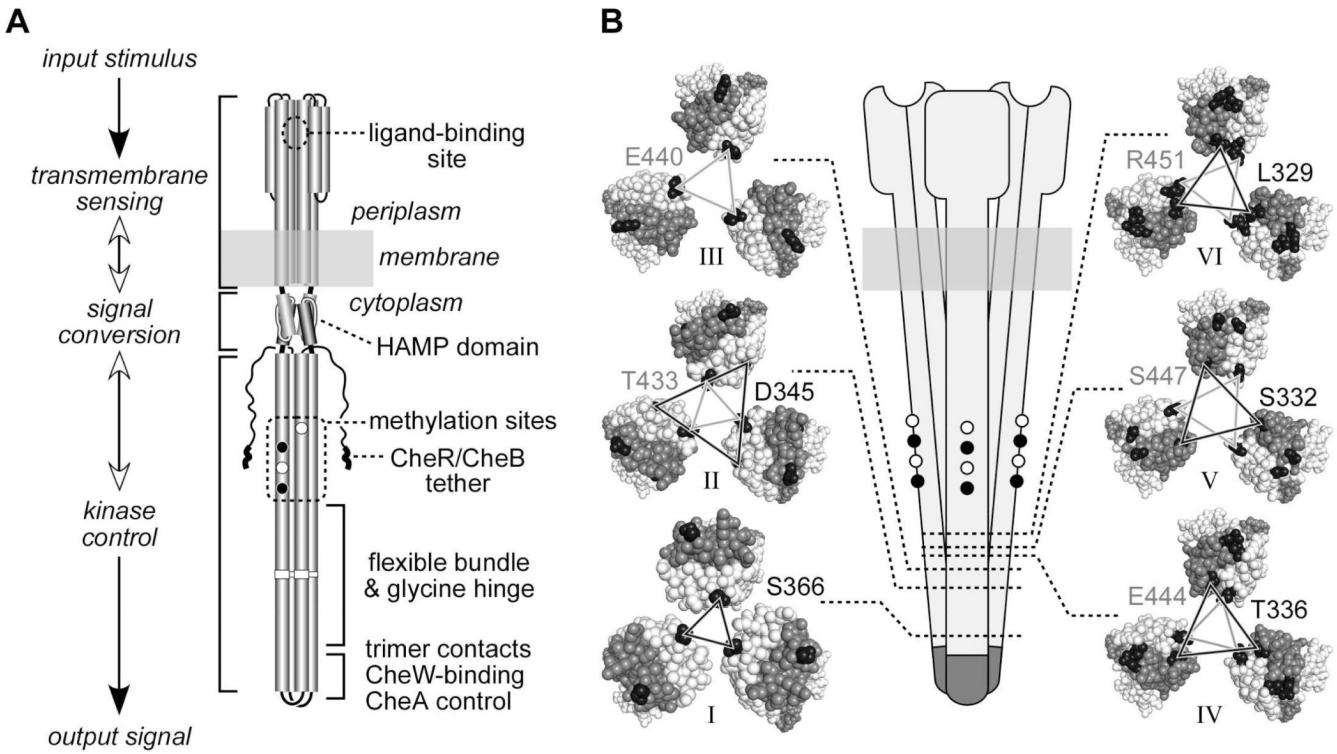

Fig. 1. Structural features of receptor molecules and trimers of dimers

A. Functional architecture of Tsr and Tar homodimers. Cylindrical segments represent alpha-helices. Black circles represent methyl-accepting residues that are translated as glutamines, then deamidated to glutamate by CheB. CheR-CheB tether represents the C-terminal region to which the methylation enzymes bind.

B. Schematic representation of a trimer of dimers (center) and cross sections corresponding to the six levels, indicated by dotted lines and roman numbers, defined in Table 1. Cross section images were made with Pymol, viewing the trimer of dimers from the cytoplasm towards the membrane. Residues between the cytoplasmic tip and the corresponding level are hidden. Axial subunits (subunits that face the interior of the trimer at level I) are colored light gray; peripheral subunits are colored dark gray. Representative residues from each level that were substituted by cysteine residues are colored black. Lines connecting the cysteine-substituted residues are black when the residues reside in the N-helix of the subunit (helix running from the membrane to the cytoplasmic tip), and gray when the residues reside in the C-helix of the subunit (helix running from the cytoplasmic tip to the C-terminus). Residue identification uses a matching shading scheme and Tsr residue numbers, even though some replacements were made in Tar (see text and Table 1).

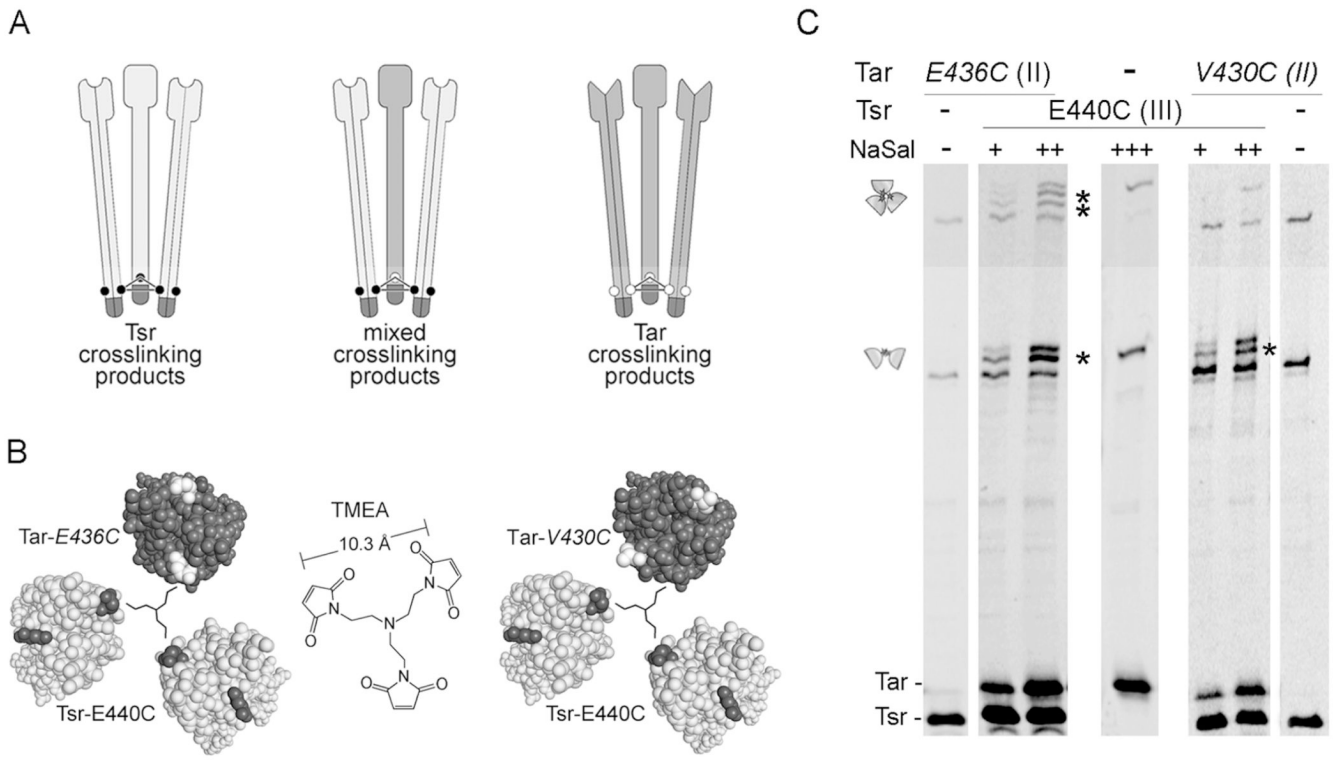

Fig. 2. Inter-receptor crosslinking tests with proximal reporter sites

A. Schematic representation of a crosslinking experiment in which two different receptors bear cysteine reporters at the same or closely adjacent levels. Individual dimers represent Tsr (light gray) or Tar (dark gray) molecules; small circles represent cysteine replacements. The three dimers form trimers through interactions between their tips (dark region). Upon TMEA treatment, cells expressing both receptor types can form pure 3-subunit crosslinking products (Tsr-only, left; Tar-only, right) and may also form mixed crosslinking products (center), if the reporter sites are sufficiently close to one another.

B. Cross section views of mixed trimers bearing reporters in adjacent levels. Left: Tar *436C* (level II), Tsr 440C (level III). Right: Tar *430C* (level II), Tsr 440C (level III). Cross section images were made with Pymol, viewing the trimer of dimers from the cytoplasm towards the membrane. Residues between the cytoplasmic tip and the corresponding level are hidden. Tsr subunits are light gray, with the cysteine reporters black. Tar subunits are dark gray, with the cysteine reporters white. A schematic representation of the TMEA crosslinking reagent (center) is shown to scale in the center of each trimer.

C. UU1581 cells carrying pCS12 Tsr-E440C and pPA818 Tar-6his-*E436C* or pPA818 Tar-6his-*V430C* were grown to mid-log phase and treated with TMEA. Tar expression was induced at 10 μM IPTG and Tsr expression at 0.15 (+), 0.30 (++), or 0.60 (+++) μM sodium salicylate. Cells expressing each receptor individually were also included to show the mobility of the pure crosslinking products. Samples were analyzed by SDS-PAGE in long, 9% acrylamide gels, and visualized by immunoblotting with an anti-Tsr antibody that reacts with both receptors. Cartoons on the left indicate the region of the gel where 2- and 3-subunit crosslinking products are found. Mixed crosslinking products are indicated with asterisks.

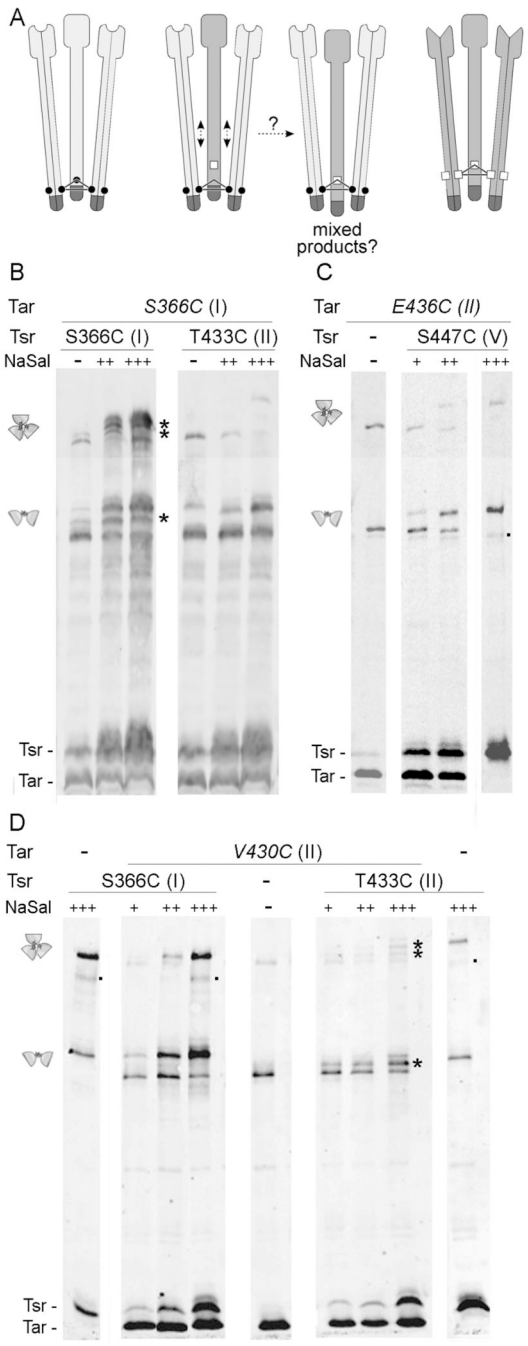

Fig. 3. Inter-receptor crosslinking between reporters located at distant levels

A. Schematic representation of a crosslinking experiment in which two different receptors bear cysteine reporters at distant levels. Individual dimers represent Tsr (light gray) or Tar (dark gray) molecules, as in Fig. 2A. Cysteine substitutions on Tsr are represented by small circles, and those on Tar by small squares, situated at a different level. TMEA treatment of cells expressing Tsr molecules bearing a cysteine residue at one level, and Tar molecules bearing a cysteine reporter at a different level will only give crosslinking products of the pure type (Tsr- or Tar-only) unless a displacement of some dimer with respect to the others occurs along the central axis of the trimer.

B–D. Strains expressing single cysteine-substituted Tar and Tsr receptors, and lacking other chemotaxis proteins, were treated with TMEA, analyzed by SDS-PAGE in long, 9% acrylamide gels, and visualized by immunoblotting with an anti-Tsr antibody that reacts with both receptors. Tsr expression was induced at 0 (−), 0.15 (+), 0.30 (++) or 0.60 (+++) μM sodium salicylate. Tar expression, when driven from the pPA818 derivatives, was induced at 10 μM IPTG. Mixed crosslinking products are indicated with asterisks. Small dots on the right side of some lanes indicate crossreacting proteins or receptor degradation products.

B. UU1613 cells (carrying a chromosomal copy of Tar-*S366C* under native promoter control) transformed with pCS12 Tsr-S366C or pCS12 Tsr-T433C were grown to mid-log phase under different induction conditions and treated with the TMEA crosslinker.

C. UU1581 cells carrying pPA818 Tar-6his-*V430C* and pCS12 Tsr-S366C or pCS12 Tsr-T433C were grown to mid-log phase under different induction conditions and treated with TMEA.

D. UU1581 cells carrying pPA818 Tar-6his-*E436C* and pCS12 Tsr-S447C were grown to mid-log phase under different induction conditions and treated with TMEA.

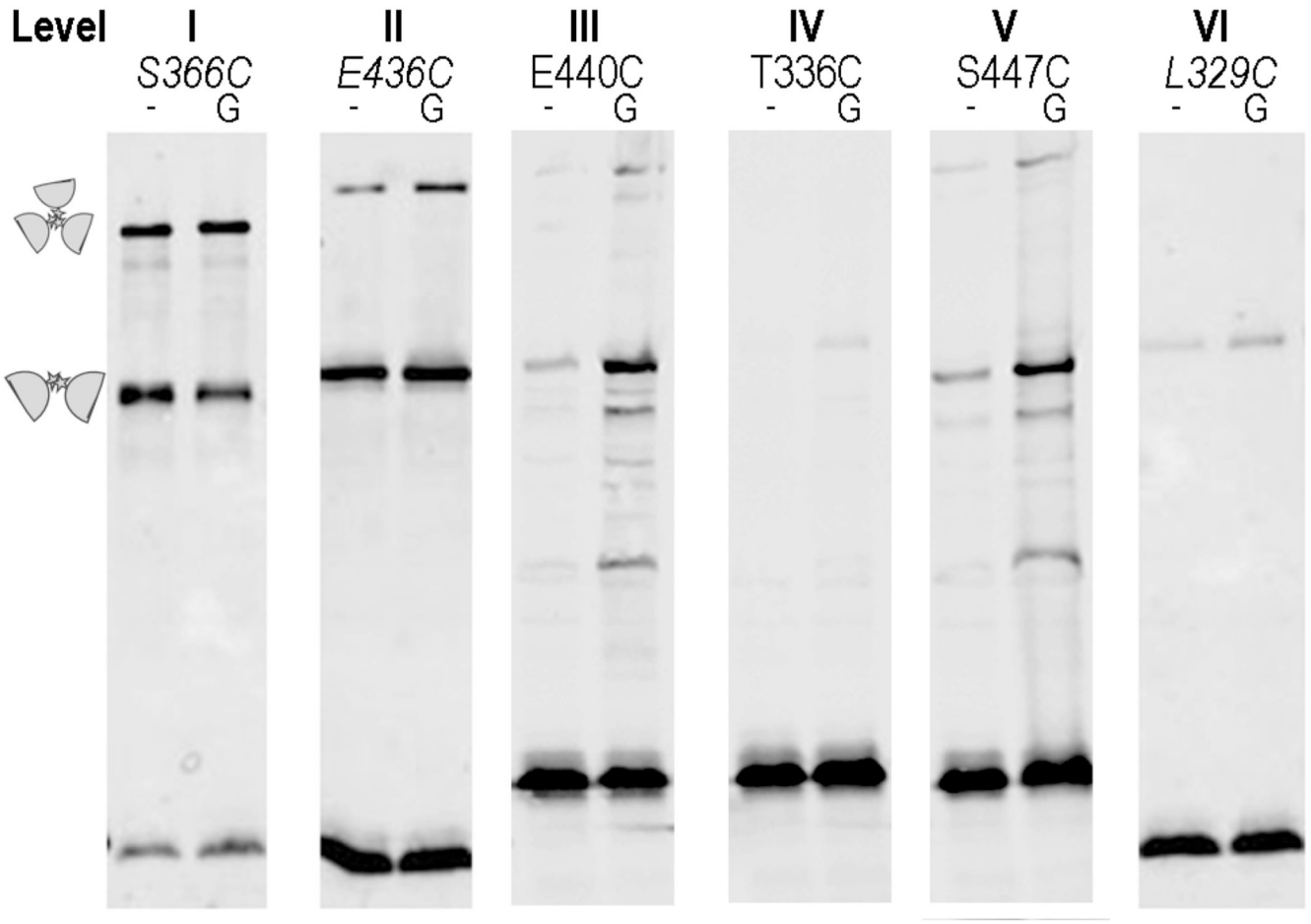

Fig. 4. Effect of glycerol stimulation on crosslinking efficiency

UU1581 cells carrying pPA818 (Tar-6his) or pCS12 (Tsr) derivatives with single-cysteine substitutions were grown to mid-log phase under conditions of physiological induction of receptors (10 μM IPTG for Tar and 0.45 μM sodium salicylate for Tsr), washed twice and resuspended in phosphate buffer. TMEA treatment was performed 10 seconds after adding water (−) or 1 M glycerol (G) to the cell suspension.

Biochemistry. Author manuscript; available in PMC 2012 February 8.

Table 1

Crosslinking efficiency of reporters located along the cytoplasmic domain

Strain UU1581 cells expressing cysteine-substituted Tsr or Tar receptors at physiological levels were treated with TMEA and the crosslinking products were analyzed by western blotting with an anti-Tsr antibody that reacts with both receptors.

Level	Distance from the tip (Å)[a]	Position[b]	Receptor	% 3-subunit product[c]	Cα-Cα (Å)[d]	Subunit[e]	Helix[e]
I	37	S366	Tsr/Tar	100	12.86	Axial	N
II	60.5	V430 (T)	Tar	11 ± 7	19.33	Axial	C
	63	T433	Tsr	23 ± 5	16.86	Axial	C
	67	E436	Tar	14 ± 3	20.65	Axial	C
	69	D345	Tar	0	32.09	Axial	N
III	74	E440	Tsr	19 ± 4	20.83	Axial	C
IV	81	T336	Tsr	1 ± 1	27.27	Peripheral	N
	81	E444 (N)	Tar	4 ± 3	22.17	Axial	C
V	87	S447 (N)	Tsr	12 ± 3	25.28	Axial	C
	87	S332	Tar	5 ± 3	28.21	Peripheral	N
VI	92	L329	Tar	1 ± 0.5	26.67	Peripheral	N
	93	R451	Tsr	1 ± 1	28.68	Axial	C
	96	Q325	Tar±	3 ± 1	26.81	Peripheral	N

[a] Distance measured from the alpha-carbon of the corresponding residue to the alpha-carbon of G390, located at the cytoplasmic tip.

[b] Residue numbering corresponds to Tsr. When a cysteine replacement was made in Tar at the equivalent position, the actual residue that was replaced is indicated between parentheses (if different from the corresponding Tsr residue).

[c] The fraction of 3-subunit crosslinking products was calculated relative to that obtained with the S366C reporter.

[d] Distance measured between alpha-carbons of the corresponding residues in subunits that face the trimer axis.

[e] Subunits and helices are defined as in Fig. 1.

Table 2

Crosslinking between cysteine reporters located at close or distant levels in different receptors

UU1581 cells expressing cysteine-substituted Tsr and Tar receptors at physiological levels were treated with TMEA and the crosslinking products were analyzed by immunoblotting with an anti-Tsr antibody that reacts with both receptors.

Position in Tar	Position in Tsr	Distances [a]	Tar-Tsr mixed crosslinking products [b]	
			2-subunits	3-subunits
436 (II)	440 (III)	20.97, 22.73	+	+
430 (II)	440 (III)	19.41, 26.72	+	−
366 (I)	433 (II)	30.61, 31.50	−	−
430 (II)	366 (I)	27.08, 29.82	−	−
436 (II)	447 (V)	27.62, 30.75	−	−

[a] The table summarizes the distances between the alpha carbon from the corresponding residue in Tar to each of the alpha carbon residues in two differently substituted Tsr dimers in a mixed trimer.

[b] The actual results of the corresponding experiments are shown in Figs. 2 and 3 and the presence of mixed crosslinking products summarized here.